Desalination and Water Treatment
www.deswater.com

doi: 10.1080/19443994.2013.833872

52 (2014) 7784–7796
December

Taylor & Francis
Taylor & Francis Group

Primary–secondary amino silica nanoparticle: synthesis and dye removal from binary system

Niyaz Mohammad Mahmoodi*, Adonis Maghsoudi, Farhood Najafi, Mojtaba Jalili, Hojjat Kharrati

Department of Environmental Research, Institute for Color Science and Technology, Tehran, Iran
Tel. +98 021 22969771; Fax: +98 021 22947537; emails: mahmoodi@icrc.ac.ir; nm_mahmoodi@aut.ac.ir; nm_mahmoodi@yahoo.com

Received 6 April 2013; Accepted 4 August 2013

ABSTRACT

In this paper, primary–secondary amino silica nanoparticle (PSASN) was synthesized, and its dye removal ability from single and binary systems containing printing dyes was investigated. The synthesized PSASN was characterized by means of Fourier transform infrared (FTIR), scanning electron microscopy (SEM), and BET analyses. Acid blue 92 (AB92), Direct Black 22 (DB22), Direct Red 31 (DR31), and Direct Red 80 (DR80) were used. The kinetics and isotherm of dye adsorption were studied. The effects of PSASN dosage, pH, salt, and initial dye concentration on dye removal were evaluated. Adsorption kinetic was found to conform to pseudo-second-order kinetics. The maximum dye adsorption capacity (Q_0) of PSASN for AB92, DB22, DR31, and DR80 were 113.636, 37.453, 114.943, and 41.152 mg/g, respectively. It was found that dye adsorption on PSASN followed Langmuir isotherm. The results showed that the PSASN as an adsorbent with dye adsorption capacity might be a suitable alternative to remove dyes from colored printing wastewater.

Keywords: Primary–secondary amino silica nanoparticle; Synthesis; Dye removal; Binary system; Printing wastewater

1. Introduction

Several industries such as printing, textile, paper, etc. use dyes. About 15% of the total annual production of dyes is lost during dyeing process which is released in wastewaters [1–7].

Adsorption process as a physical treatment is widely used to remove pollutants from wastewater [8]. Some of adsorbents have some disadvantages such as relatively limited adsorption capacity, poor mechanical, and heat resistance [9]. Silica as an adsorbent is of particular interest because of its stability and possible reuse [10]. In addition silica is a modifiable material [11]. The modified silica has new surface functional groups and is capable to adsorb various organic compounds [12]. Several functional groups have been introduced to silica [9,10,13–19]. However, the synthesis procedures of the surface-modified adsorbents (SMA) are much complex and expensive [15]. Therefore, it is necessary to design a SMA by a simple and cost-effective process.

A literature review showed that primary–secondary amino silica nanoparticle (PSASN) was not used to remove dyes from binary system (Fig. 1). In this paper, PSASN was synthesized, and its dye removal

*Corresponding author.

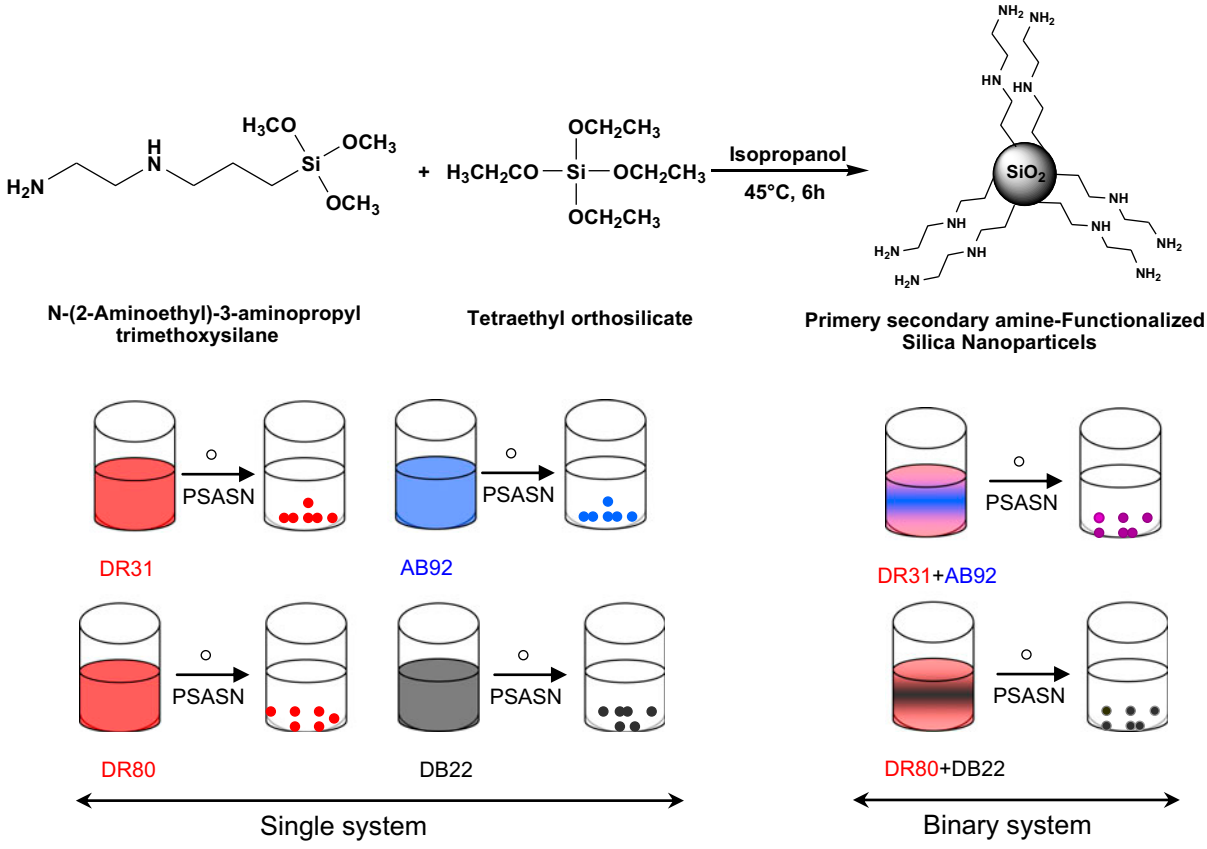

Fig. 1. The synthesis of PSASN and its dye removal ability from single and binary systems.

ability from single and binary systems containing printing dyes was studied. Acid blue 92 (AB92), Direct Black 22 (DB22), Direct Red 31 (DR31), and Direct Red 80 (DR80) were used as model compounds. The physical characteristics of PSASN were investigated. The kinetic and isotherm of dye adsorption were studied in details. The effects adsorbent dosage, initial dye concentration, pH, and salt as operational parameters on dye removal were evaluated.

2. Materials and methods

2.1. Chemicals

Acid blue 92 (AB92), Direct Black 22 (DB22), Direct Red 31 (DR31), and Direct Red 80 (DR80) were achieved from Ciba and used without further purification. The chemical structure of dyes was shown in Fig. 2. All other chemicals were of analytical grade and obtained from Merck.

2.2. Synthesis of PSASN

The PSASN was synthesized by tetra ethyl orthosilicate (TEOS, 0.12 mol, 25 g) and N-(2-aminoethyl)-3-aminopropyl trimethoxysilane (0.07 mol, 15 g) in isopropyl alcohol (60 mL) as a solvent and water (5 g) as hydrolyzing agent at 45 ℃ for 6 h under N_2 inert gas. Then, PSAS was filtered and dried at 90 ℃ for 4 h. The weight of PSAS was 17 g (yield, 93%) (Fig. 1).

2.3. Characterization of PSASN

Fourier transform infrared (FTIR) spectrum (Perkin–Elmer spectrophotometer spectrum one) of PSASN in the range 4,000–450 cm^{-1} was studied. The morphological structure of the PSASN was examined by scanning electron microscopy (SEM) using LEO 1455VP scanning microscope.

The specific surface area of PSASN was evaluated through N_2 adsorption at 77 K, using an Autosorb1-Quantachrome instrument. The BET (Brunauer–Emmet–Teller) model was applied.

The pH of PSASN point of zero charge (pH_{PZC}) was determined. To determine the pH_{PZC}, 0.1 g of adsorbent was added to 100 mL of water with varying pH from 2 to 11 and stirred for 24 h [20]. Final pH of the solution was plotted against initial pH of the solution. pH_{PZC} for PSASN is determined pH 6.0 (Fig. 3).

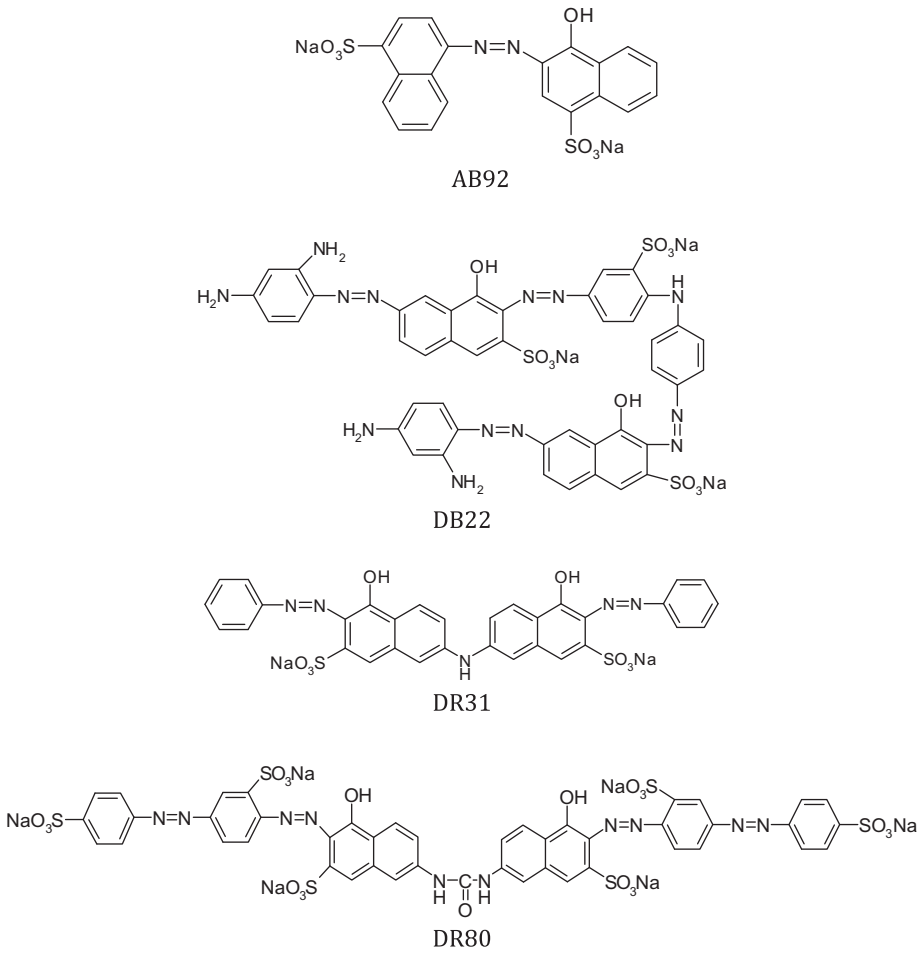

Fig. 2. The chemical structure of dyes.

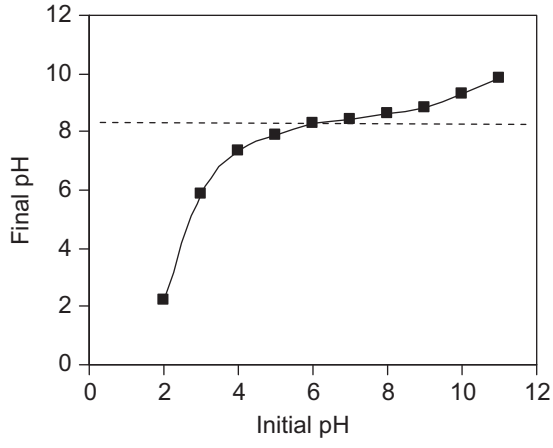

Fig. 3. The pH of PSASN point of zero charge (pH_{PZC}).

2.4. Adsorption procedure

The dye adsorption measurements were conducted by mixing of PSASN and dye in jars containing 250 mL of a dye solution (50 mg/L). The solution pH was adjusted by adding a small amount of H_2SO_4 or NaOH. The absorbance of all solution samples was measured at certain time intervals during the adsorption process. At the end of the adsorption experiments, the solution samples were centrifuged and the dye concentration was determined.

UV–vis Perkin–Elmer Lambda 25 spectrophotometer was used for absorbance measurement of samples. The maximum wavelength (λ_{max}) used for determination of residual concentration of AB92, DB22, DR31, and DR80 at pH 2 in supernatant solution using UV–vis spectrophotometer were 571, 470, 530, and 523 nm, respectively.

The effect of PSASN dosage (0.01–0.07 g) on dye removal was investigated by contacting 250 mL of dye solution with initial dye concentration of 50 mg/L and pH 2 using jar test at room temperature (25˚C) for 60 min at a constant stirring speed of 200 rpm.

The effect of pH (2, 5, 8, and 10) on dye removal was investigated by contacting 250 mL of dye solution with PSASN and initial dye concentration (50 mg/L)

using jar test at room temperature (25°C) for 60 min at a constant stirring speed of 200 rpm.

The effect of salt (0.02 mol) on dye removal was investigated by contacting 250 mL of dye solution (50 mg/L) with PSASN and pH 2 using jar test at room temperature (25°C) for 60 min at a constant stirring speed of 200 rpm. Different salts ($NaHCO_3$, Na_2CO_3, and Na_2SO_4) were used.

The effect of initial dye concentration (25, 50, 75, and 100 mg/L) on dye removal was investigated by contacting 250 mL of dye solution with PSASN and pH 2 using jar test at room temperature (25°C) for 60 min at a constant stirring speed of 200 rpm.

Dye concentrations were calculated as follows. For a binary system, components A and B were measured at λ_1 and λ_2, respectively, to give optical densities of d_1 and d_2 [4]:

$$C_A = (k_{B2} \times d_1 - k_{B1} \times d_2)/(k_{A1} \times k_{B2} - k_{A2} \times k_{B2}) \quad (1)$$

$$C_B = (k_{A1} \times d_2 - k_{A2} \times d_1)/(k_{A1} \times k_{B2} - k_{A2} \times k_{B2}) \quad (2)$$

where k_{A1}, k_{B1}, k_{A2}, and k_{B2} are the calibration constants for components A and B at the two wavelengths λ_1 and λ_2, respectively.

3. Results and discussion

3.1. Characterization of PSASN

The FTIR spectrum of the PSASN was shown in Fig. 4. The N–H stretching vibration of primary and secondary amines is as broad band at 3,400–3,200 cm^{-1}. The C-H stretching vibration of CH_2 units in aminosilane was in 2,940 cm^{-1}. The N-H deformation vibration of NH_2 groups was in 1,484 cm^{-1}. Bending vibration of CH_2 was in 1,484 cm^{-1}. The C-N stretching vibration was between 1,321 and 1,150 cm^{-1}. The Si-O stretching vibration of silica was as a wide and strong absorption in 1,046 cm^{-1}. In addition, FTIR spectrum displays a number of characteristic bands at 957 cm^{-1} and 801 cm^{-1}. These bands are assigned to stretching vibration of υ(≡Si–O–Si≡) of siloxane backbone and υ(≡Si–OH) of free silanol group and tetrahedron ring υ (SiO_4), respectively [9,13,14,16,21,22]. The spectrum also displays a strong band at 470 cm^{-1} which is assigned to υ(≡Si–O–Si≡) deformation [22].

SEM has been a primary tool for characterizing the surface morphology and fundamental physical properties of the adsorbent surface. It is useful for determining the particle shape and appropriate size distribution of the adsorbent. Scanning electron micrograph of PSASN is shown in Fig. 5.

The surface area (S_{BET}) of the silica nanoparticle and PSASN was 110 and 93 m^2/g, respectively. Amine functional group reduces the BET surface area of silica nanoparticle.

3.2. Adsorption kinetic

The mechanism of pollutant adsorption onto an adsorbent can be investigated using kinetic studies. In order to investigate the mechanism of adsorption, characteristic constants of adsorption were determined using intraparticle diffusion [23–25], pseudo-first-order equation [26], and pseudo-second-order equation [27].

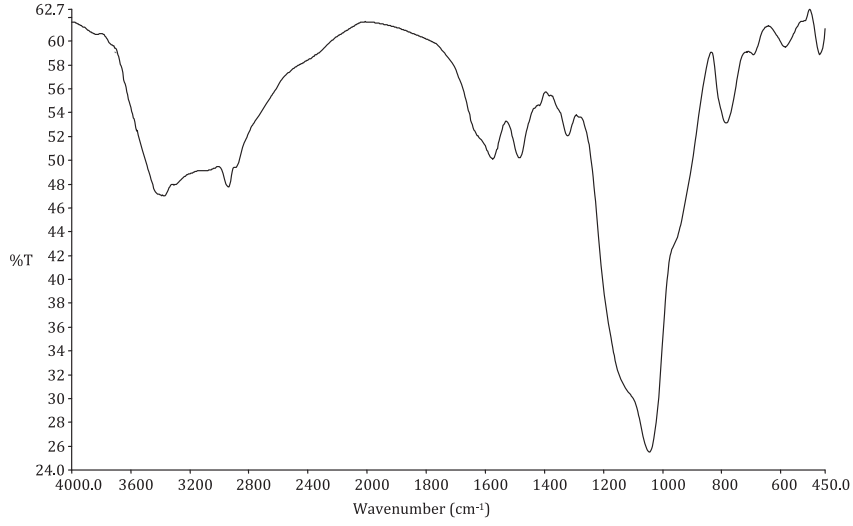

Fig. 4. FTIR spectrum of PSASN.

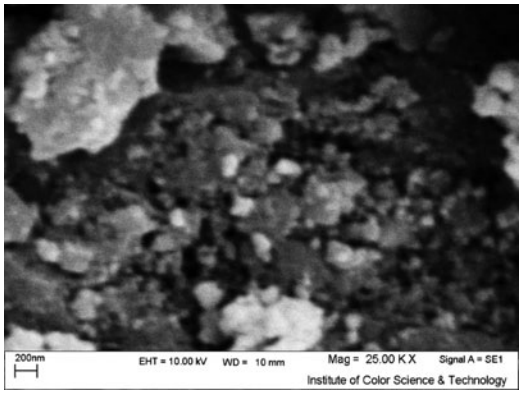

Fig. 5. The SEM image of PSASN.

A linear form of pseudo-first-order model is:

$$\log(q_e - q_t) = \log(q_e) - (k_1/2.303)t \quad (3)$$

where q_e, q_t, and k_1 are the amount of dye adsorbed on PSASN at equilibrium (mg/g), the amount of dye adsorbed at time t (mg/g), and the equilibrium rate constant of pseudo-first-order kinetics (1/min), respectively.

Linear form of pseudo-second-order model was illustrated as:

$$t/q_t = 1/k_2 q_e^2 + (1/q_e)t \quad (4)$$

where k_2 is the equilibrium rate constant of pseudo-second order (g/mg min).

The possibility of intraparticle diffusion resistance affecting adsorption was explored by using the intraparticle diffusion model as

$$q_t = k_p t^{1/2} + I \quad (5)$$

where k_p and I are the intraparticle diffusion rate constant and intercept, respectively.

To understand the applicability of the pseudo-first-order, pseudo-second-order, and intraparticle diffusion models for the dye adsorption onto PSASN at different adsorbent dosages, linear plots of log $(q_e - q_t)$ vs. contact time (t), t/q_t vs. contact time (t), and q_t against $t^{1/2}$, are plotted. The values of k_1, k_2, k_p, I, R^2 (correlation coefficient), and the calculated q_e ($(q_e)_{\mathrm{Cal.}}$) are shown in Table 1. The linearity of the plots (R^2) demonstrates that intraparticle diffusion and pseudo-first-order kinetic models do not play a significant role in the uptake of the dye by PSASN (Table 1). The linear fit between the t/q_t vs. contact time (t) and calculated correlation coefficients (R^2) for pseudo-second-order kinetics model show that the dye removal kinetic can be approximated as pseudo-second-order kinetics (Table 1). In addition, the experimental q_e ($(q_e)_{\mathrm{Exp.}}$) values agree with the calculated ones ($(q_e)_{\mathrm{Cal.}}$), obtained from the linear plots of pseudo-second-order kinetics (Table 1).

3.3. Adsorption isotherm

Several isotherms such as Langmuir, Freundlich, and Tempkin models were investigated in details.

The Langmuir isotherm can be used to explain the adsorption of dye onto adsorbent. A basic assumption of the Langmuir theory is that adsorption takes place at specific sites within the adsorbent [28–30]. The Langmuir equation can be written as follows:

$$q_e = Q_0 K_L C_e / 1 + K_L C_e \quad (6)$$

where C_e, K_L, and Q_0 are the equilibrium concentration of dye solution (mg/L), Langmuir constant (L/g), and the maximum adsorption capacity (mg/g), respectively.

The linear form of Langmuir equation is:

$$C_e/q_e = 1/K_L Q_0 + C_e/Q_0 \quad (7)$$

In addition, isotherm data were tested with Freundlich isotherm that can be expressed by [31]:

$$q_e = K_F C_e^{1/n} \quad (8)$$

where K_F is adsorption capacity at unit concentration and $1/n$ is adsorption intensity.

The $1/n$ values indicate the type of isotherm to be irreversible ($1/n = 0$), favorable ($0 < 1/n < 1$), and unfavorable ($1/n > 1$). Eq. (8) can be rearranged to a linear form:

$$\log q_e = \log K_F + (1/n)\log C_e \quad (9)$$

Tempkin isotherm assumes that the heat of adsorption of all the molecules in the layer decreases linearly with coverage due to adsorbent–adsorbate interactions. Also, the adsorption in Tempkin isotherm is characterized by a uniform distribution of binding energies, up to some maximum binding energy [32,33]. The Tempkin isotherm is given as:

$$q_e = RT/b \ln(K_T C_e) \quad (10)$$

which can be linearized as:

$$q_e = B_1 \ln K_T + B_1 \ln C_e \quad (11)$$

Table 1
Linearized kinetic coefficient for dye adsorption onto PSASN at different adsorbent dosages from single and binary systems

System		Dosage (g)	(q_e) Exp	Pseudo-first order			Pseudo-second order			Intraparticle diffusion		
				$(q_e)_{Cal.}$	k_1	R^2	$(q_e)_{Cal}$	k_2	R^2	k_P	I	R^2
Single		AB92										
		0.050	100.750	45.793	0.046	0.979	104.167	0.002	0.994	6.493	51.435	0.984
		0.100	85.300	26.693	0.042	0.975	86.207	0.005	0.997	3.868	55.670	0.986
		0.150	72.433	17.010	0.063	0.988	73.529	0.010	0.999	2.470	55.067	0.933
		0.200	57.938	2.712	0.036	0.920	57.803	0.056	0.999	0.424	54.654	0.917
		DR31										
		0.050	98.650	40.059	0.049	0.948	101.010	0.003	0.996	5.422	57.337	0.985
		0.100	80.600	23.437	0.042	0.984	81.967	0.006	0.998	3.300	54.946	0.986
		0.150	66.97	11.013	0.036	0.988	67.114	0.012	0.9991	1.616	54.195	0.986
		0.200	57.163	2.752	0.054	0.936	57.143	0.065	1.000	0.410	54.199	0.913
		DR80										
		0.100	39.750	8.590	0.055	0.968	38.911	0.016	0.996	1.126	29.864	0.912
		0.200	36.875	8.080	0.047	0.809	37.037	0.018	0.998	1.061	28.602	0.945
		0.300	31.985	7.681	0.020	0.914	31.746	0.021	0.998	0.794	25.186	0.963
		0.400	30.094	5.711	0.027	0.944	30.675	0.017	0.999	1.154	21.548	0.987
		DB22										
		0.100	36.625	17.632	0.045	0.960	38.023	0.006	0.981	2.344	18.274	0.978
		0.200	32.125	12.151	0.038	0.881	32.573	0.009	0.991	1.574	19.220	0.967
		0.300	28.917	11.647	0.079	0.947	29.851	0.014	0.998	1.328	19.371	0.969
		0.400	26.313	5.948	0.059	0.965	26.738	0.027	0.999	0.929	19.795	0.895
Binary	AB92	AB92										
	+DR31	0.050	48.863	21.208	0.043	0.966	50.251	0.005	0.995	3.169	24.867	0.951
		0.100	43.279	20.936	0.056	0.984	45.249	0.006	0.998	2.976	21.732	0.963
		0.150	33.258	11.288	0.045	0.981	33.898	0.011	0.998	1.614	20.873	0.975
		0.200	27.319	4.977	0.041	0.954	27.473	0.028	0.999	0.764	21.515	0.946
		DR31										
		0.050	44.250	32.374	0.044	0.9866	48.780	0.002	0.984	4.538	9.430	0.996
		0.100	41.856	21.642	0.055	0.9946	44.903	0.005	0.997	3.043	19.655	0.975
		0.150	33.500	11.574	0.052	0.9899	34.274	0.011	0.999	1.586	22.891	0.969
		0.200	27.697	5.314	0.041	0.9790	27.855	0.026	0.999	0.790	21.658	0.978
	DR80	DR80										
	+DB22	0.100	21.400	7.024	0.030	0.965	21.459	0.015	0.992	0.958	13.291	0.958
		0.200	19.794	6.571	0.055	0.987	20.202	0.019	0.998	0.952	12.656	0.974
		0.300	16.610	3.045	0.062	0.993	16.807	0.057	0.999	0.434	13.538	0.938
		0.400	14.419	1.931	0.054	0.929	14.514	0.081	0.999	0.248	12.535	0.976
		DB22										
		0.100	20.968	7.034	0.030	0.943	21.008	0.015	0.992	0.948	12.921	0.965
		0.200	18.600	5.884	0.044	0.879	18.868	0.021	0.996	0.753	12.592	0.981
		0.300	15.979	3.141	0.030	0.979	15.924	0.040	0.998	0.471	12.141	0.973
		0.400	13.989	2.967	0.057	0.789	14.104	0.054	0.999	0.337	11.346	0.973

where

$$B_1 = RT/b \quad (12)$$

A plot of q_e vs. $\ln C_e$ enables the determination of the isotherm constants B_1 and K_T from the slope and the intercept, respectively. K_T is the equilibrium binding constant (L/mol) corresponding to the maximum binding energy and constant B_1 is related to the heat of adsorption.

To study the applicability of the Langmuir, Freundlich, and Tempkin isotherms for the dye adsorption onto PSASN at different adsorbent dosage, linear

plots of C_e/q_e against C_e, $\log q_e$ vs. $\log C_e$, and q_e vs. $\ln C_e$ are plotted. The values of Q_0, K_L, K_F, $1/n$, K_T, B_1, and R^2 (correlation coefficient values of all isotherms models) are shown in Table 2. The correlation coefficient values (R^2) show that the dye removal isotherm using PSASN does not follow the Freundlich and Tempkin isotherms (Table 2). The linear fit between the C_e/q_e vs. C_e and calculated correlation coefficients (R^2) for Langmuir isotherm model show that the dye removal isotherm can be approximated as Langmuir model (Table 2). This means that the adsorption of dyes takes place at specific homogeneous sites and a one layer adsorption onto PSASN surface.

3.4. Operational parameter effect on dye removal

3.4.1. PSASN dosage

Dye removal at different PSASN dosages (g) was shown in Fig. 6. The increase in dye adsorption with adsorbent dosage can be attributed to increased adsorbent surface and availability of more adsorption sites. However, if the adsorption capacity was expressed in mg adsorbed per gram of material, the capacity decreased with the increasing amount of PSASN. It can be attributed to overlapping or aggregation of adsorption sites resulting in a decrease in total adsorbent surface area available to the dye and an increase in diffusion path length [34].

3.4.2. pH

The effect of pH on the adsorption of dyes onto PSASN is shown in Fig. 7. The results showed that the adsorption capacity increases when the pH is decreased. Maximum adsorption of anionic dyes occurs at acidic pH (pH 2). The electrostatic attraction as well as the organic property and structure of dye molecules and PSASN could play very important roles in dye adsorption on PSASN. At pH 2, a significantly high electrostatic attraction exists between the positively charged surfaces of the adsorbent, due to the ionization of functional groups of adsorbent and negatively charged anionic dye. As the pH of the system increases, the number of positively charged sites decreases. It does not favor the adsorption of anionic dyes due to the decreasing of electrostatic attraction [35]. The effective pH was 2 and it was used in further studies.

3.4.3. Salt (inorganic ions)

The occurrence of different salts as dissolved inorganic anions is rather common in different industrial wastewaters [36,37]. These substances may compete for the active sites on the adsorbent surface or deactivate the adsorbent and, subsequently, decrease the dye adsorption efficiency. A major drawback resulting from the high reactivity and nonselectivity of adsorbent is that it also reacts with non-target compounds present

Table 2
Linearized isotherm coefficient for dye adsorption onto PSASN at different adsorbent dosages from single and binary systems

System		Langmuir			Freundlich		Tempkin			
		Q_0	K_L	R^2	K_F	$1/n$	R^2	K_T	B_1	R^2
Single		AB92								
		113.636	0.256	0.987	41.143	0.279	0.974	4.096	21.516	0.967
		DR31								
		114.943	0.169	0.981	37.111	0.277	0.975	3.117	20.818	0.945
		DR80								
		41.152	0.529	0.992	27.689	0.0909	0.818	6063.242	3.119	0.800
		DB22								
		37.453	0.379	0.982	23.174	0.102	0.789	1914.095	3.006	0.746
Binary	AB92 + DR31	AB92								
		62.112	0.252	0.9931	18.226	0.380	0.944	2.241	14.199	0.951
		DR31								
		51.020	0.433	0.966	21.399	0.280	0.926	16.379	8.073	0.919
	DR80 + DB22	DR80								
		23.310	1.576	0.997	12.578	0.192	0.978	33.616	3.382	0.971
		DB22								
		26.247	0.437	0.997	9.931	0.221	0.987	5329.432	1.455	0.970

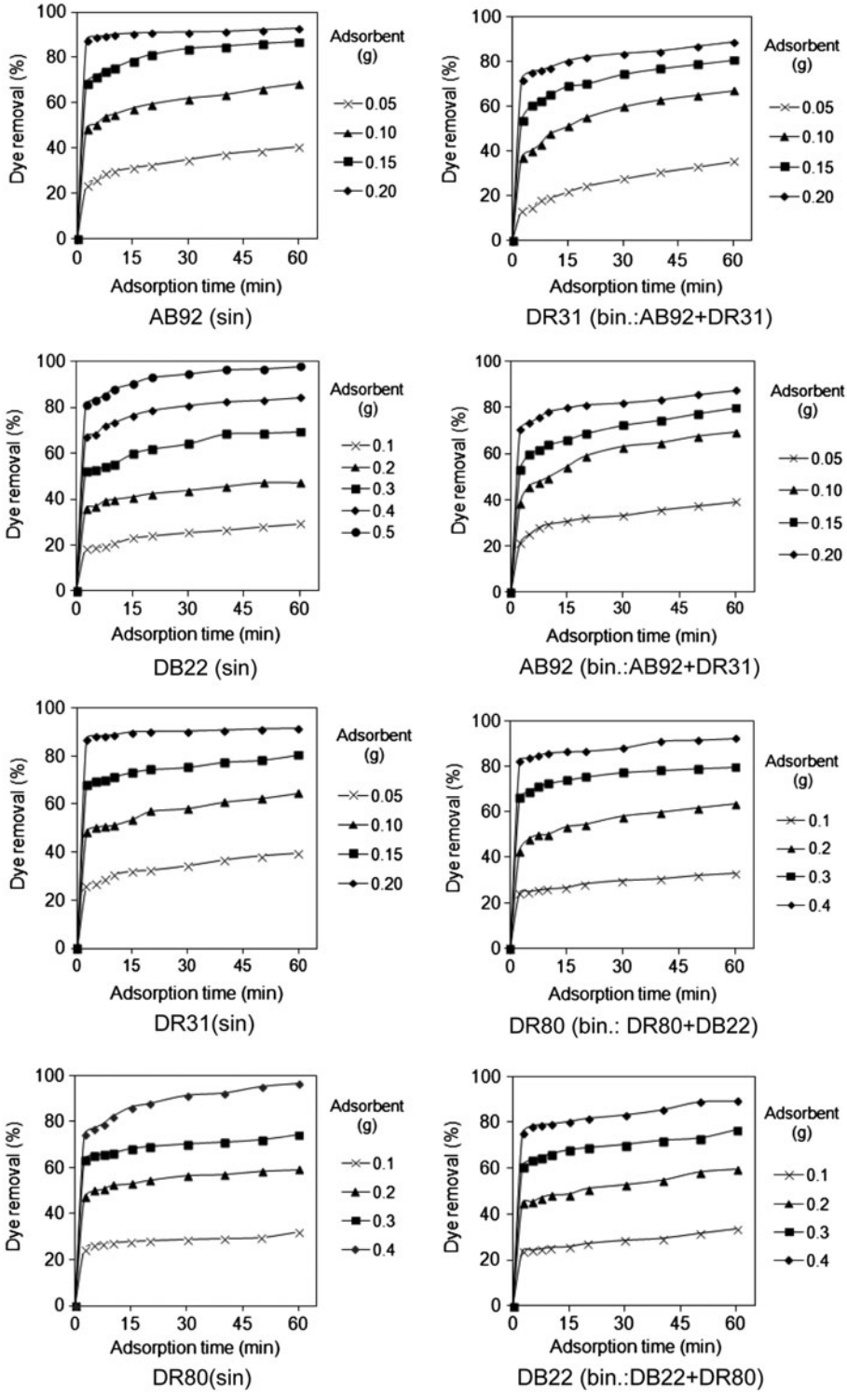

Fig. 6. The effect of adsorbent dosage on dye removal by PSASN from single and binary systems.

in the background water matrix, i.e. dye auxiliaries present in the exhausted reactive dye bath. It results higher adsorbent dosage demand to accomplish the desired degree of dye removal efficiency. Fig. 8 illustrates that dye removal capacity of PSASN decreases in the presence of inorganic salts because these salts have small molecules and compete with dyes in adsorption by PSASN.

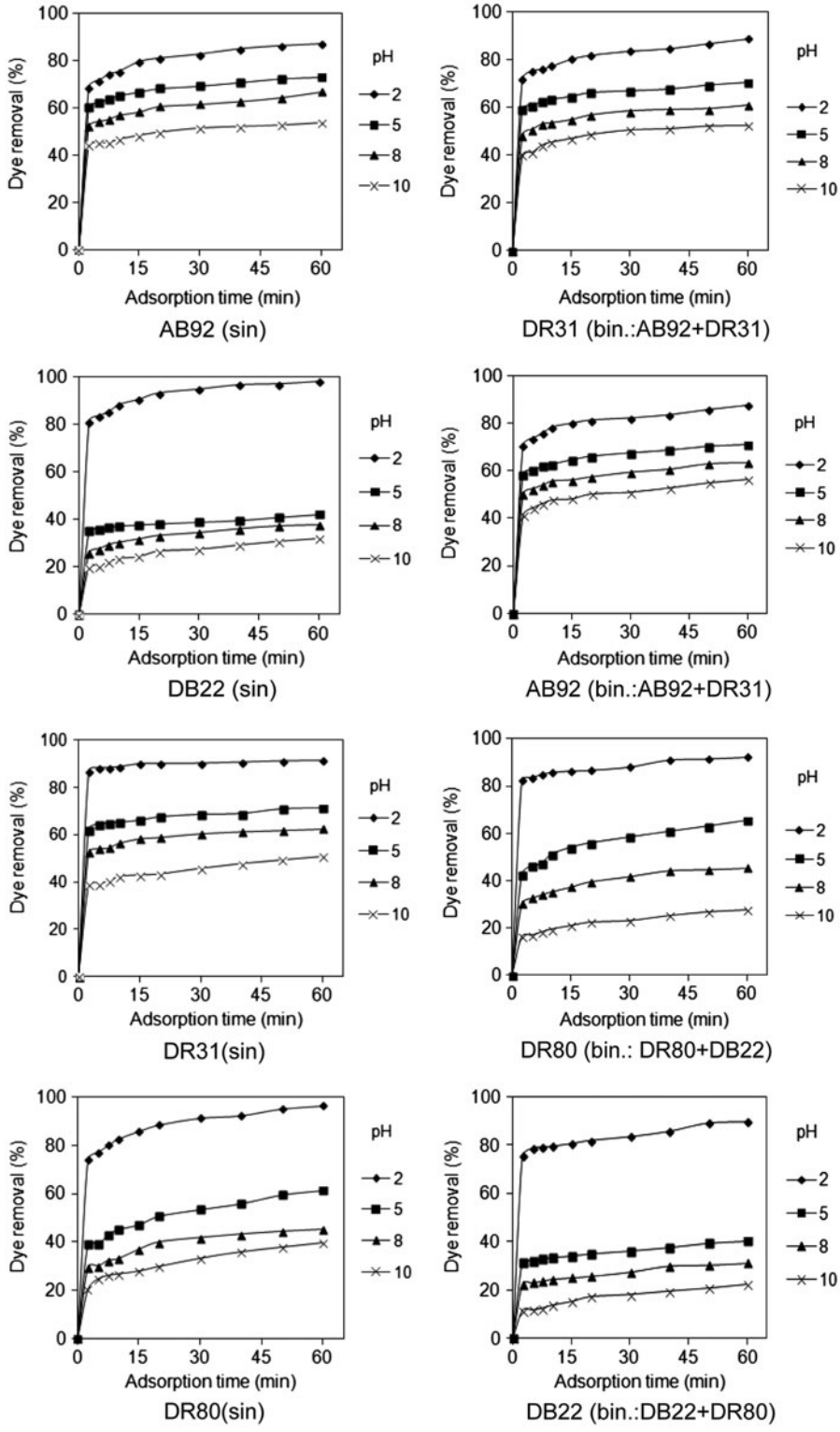

Fig. 7. The effect of pH on dye removal by PSASN from single and binary systems.

3.4.4. Dye concentration

The influence of varying the initial dye concentration of dyes on adsorption efficiencies onto PSASN was assessed. The results are shown in Fig. 9. It is obvious that the higher the initial dye concentration, the lower the percentage of dye adsorbed.

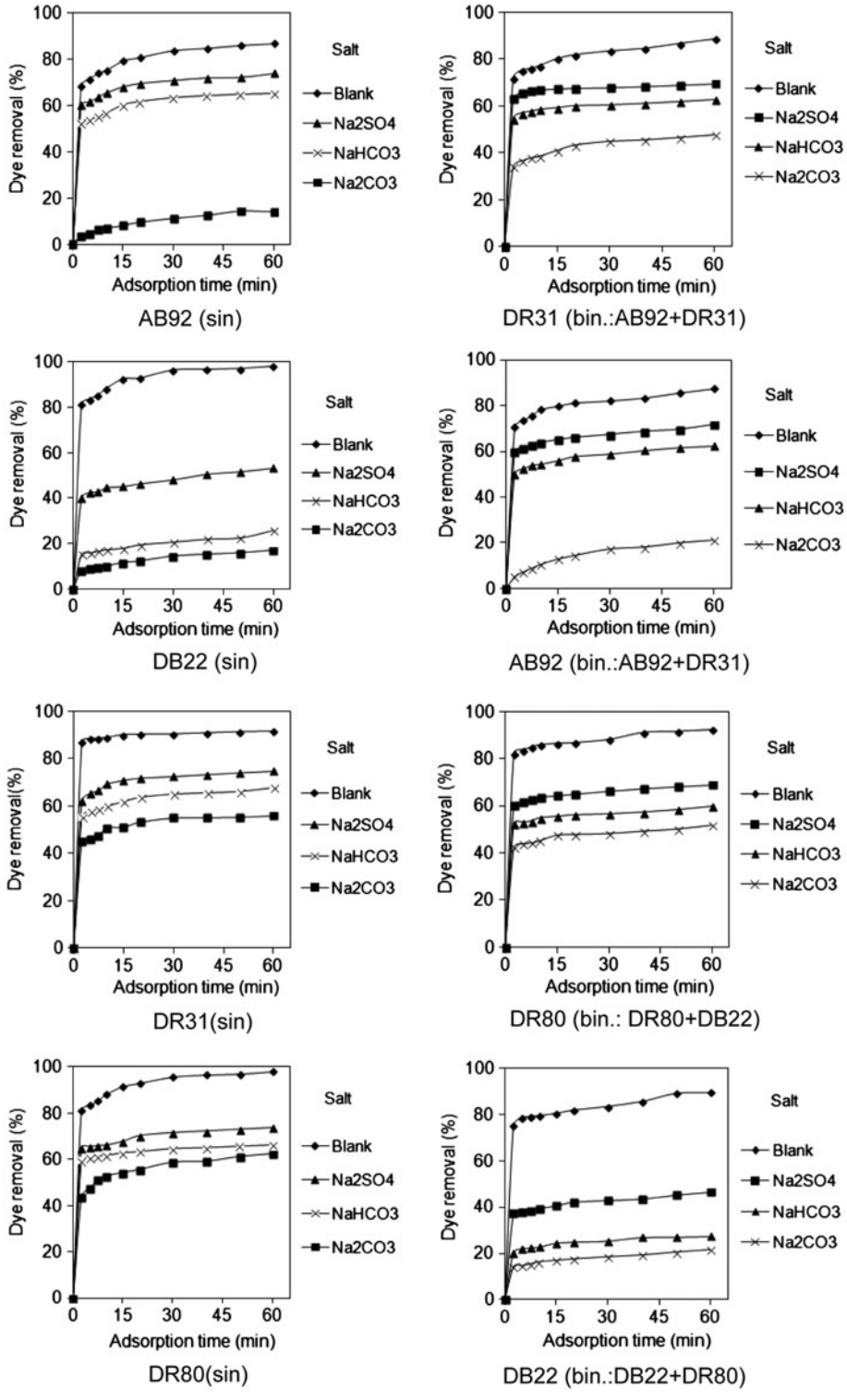

Fig. 8. The effect of salt on dye removal by PSASN from single and binary systems.

The amount of the dye adsorbed onto PSASN increases with an increase in the initial dye concentration of solution if the amount of adsorbent is kept unchanged due to the increase in the driving force of the concentration gradient with the higher initial dye concentration. The adsorption of dye by PSASN is

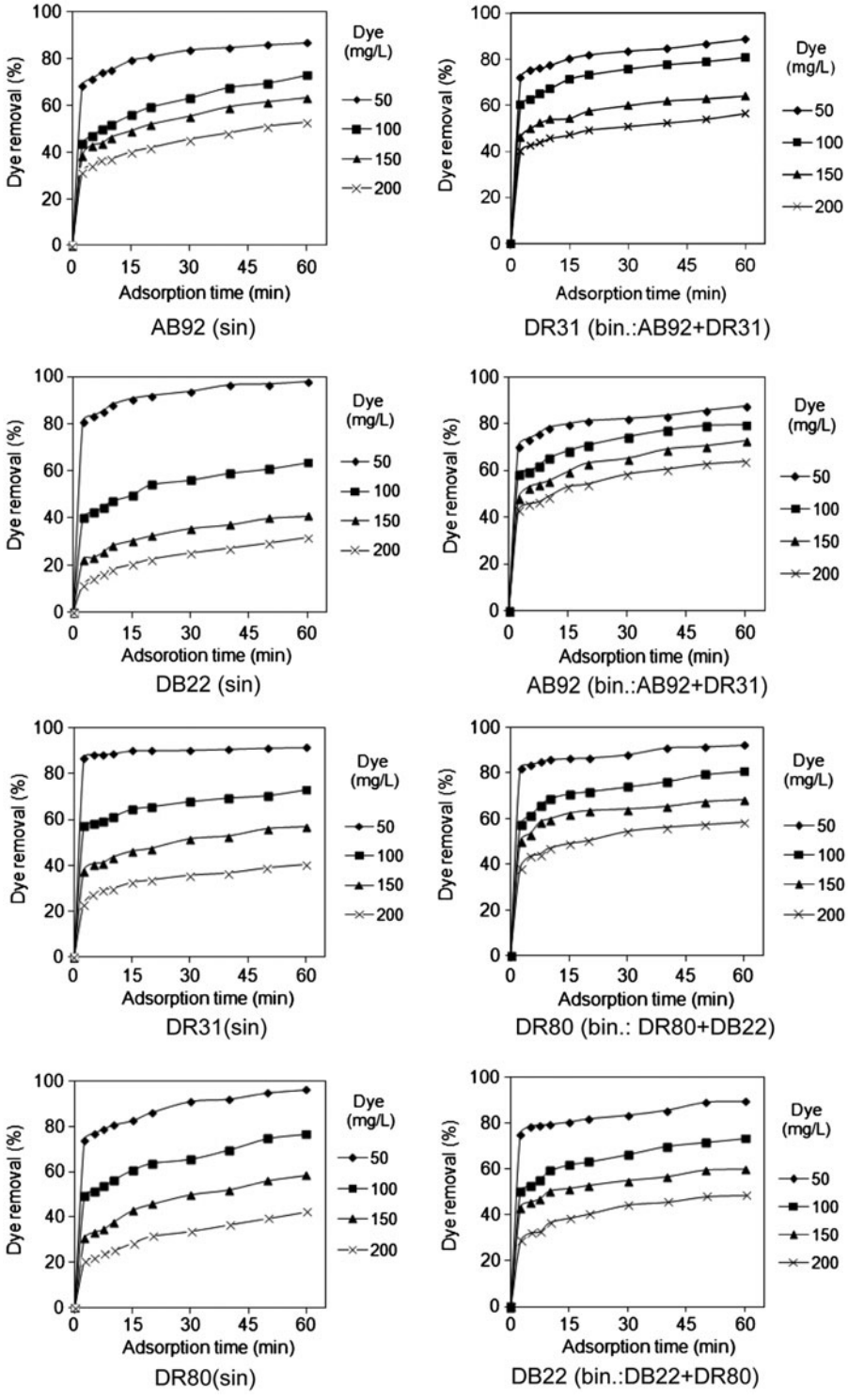

Fig. 9. The effect of dye concentration on dye removal by PSASN from single and binary systems.

very intense and reaches equilibrium very quickly at low initial concentration. At a fixed PSASN dosage, the amount of dye adsorbed increased with increasing concentration of solution, but the percentage of adsorption decreased. In other words, the residual dye concentration will be higher for higher initial dye concentrations. In the case of lower concentrations, the ratio of initial number of dye moles to the available

adsorption sites is low and subsequently the fractional adsorption becomes independent of initial concentration [38–41].

4. Conclusion

PSASN was synthesized and its dye removal ability from single and binary systems was investigated. The characteristics of PSASN were studied. Anionic dyes were used as model dyes. Dye adsorption followed Langmuir isotherm and pseudo-second-order kinetics. The dye removal increases by increasing PSASN dosage. Maximum dye adsorption occurs at acidic pH due to the protonation of amino group of adsorbent. Dye removal capacity decreases in the presence of inorganic salts. The initial dye concentration affects on adsorption efficiency of PSASN. The results showed that the PSASN as an adsorbent might be a suitable alternative to remove dyes from colored aqueous solutions.

References

[1] N.M. Mahmoodi, Photocatalytic ozonation of dyes using multiwalled carbon nanotube, J. Mol. Catal. A: Chem. 366 (2013) 254–260.

[2] N.M. Mahmoodi, Equilibrium, kinetic and thermodynamic of dye removal using alginate from binary system, J. Chem. Eng. Data. 56 (2011) 2802–2811.

[3] N.M. Mahmoodi, Photocatalytic ozonation of dyes using copper ferrite nanoparticle prepared by co-precipitation method, Desalination 279 (2011) 332–337.

[4] K.K.H. Choy, J.F. Porter, G. McKay, Langmuir isotherm models applied to the multicomponent sorption of acid dyes from effluent onto activated carbon, J. Chem. Eng. Data. 45 (2000) 575–584.

[5] M. Ghaedi, B. Sadeghian, S.N. Kokhdan, A.A. Pebdani, R. Sahraei, A. Daneshfar, A. Mihandoost, Study of removal of direct yellow 12 by cadmium oxide nanowires loaded on activated carbon, Mater. Sci. Eng. C 33 (2013) 2258–2265.

[6] M. Ghaedi, M. Ghayedi, S.N. Kokhdan, R. Sahraei, A. Daneshfar, Palladium, silver, and zinc oxide nanoparticles loaded on activated carbon as adsorbent for removal of bromophenol red from aqueous solution, J. Ind. Eng. Chem. 19 (2013) 1209–1217.

[7] M. Ghaedi, F. Karimi, B. Barazesh, R. Sahraei, A. Daneshfar, Removal of reactive orange 12 from aqueous solutions by adsorption on tin sulfide nanoparticle loaded on activated carbon, J. Ind. Eng. Chem. 19 (2013) 756–763.

[8] M. Ozacar, I.A. Sengil, Adsorption of reactive dyes on calcined alunite from aqueous solutions, J. Hazard. Mater. 9 (2003) 211–224.

[9] H. Yang, Q. Feng, Direct synthesis of pore-expanded aminofunctionalized mesoporous silicas with dimethyldecylamine and the effect of expander dosage on their characterization and decolorization of sulphonated azo dyes, Micropor. Mesopor. Mater. 135 (2010) 124–130.

[10] A.R. Cestari, E.F.S. Vieira, G.S. Vieira, L.E. Almeida, The removal of anionic dyes from aqueous solutions in the presence of anionic surfactant using aminopropylsilica—A kinetic study, J. Hazard. Mater. 138 (2006) 133–141.

[11] M.A. Hassanien, K.S. Abou-El-Sherbini, Synthesis and characterization of morin-functionalized silica gel for the enrichment of some precious metal ions, Talanta 68 (2006) 1550–1559.

[12] M. Sliwka-Kaszynska, K. Jaszczolt, A. Kolodziejczyk, J. Rachon, 1,3-alternate 25,27-dibenzoiloxy-26,28-bis-[3-propyloxy]-calix[4]arenebonded silica gel as a new type of HPLC stationary phase, Talanta 68 (2006) 1560–1566.

[13] H. Yang, Q. Feng, Characterization of pore-expanded aminofunctionalized mesoporous silicas directly synthesized with dimethyldecylamine and its application for decolorization of sulphonated azo dyes, J. Hazard. Mater. 180 (2010) 106–114.

[14] A.M. Donia, A.A. Atia, W.A. Al-amrani, A.M. El-Nahas, Effect of structural properties of acid dyes on their adsorption behaviour from aqueous solutions by amine modified silica, J. Hazard. Mater. 161 (2009) 1544–1550.

[15] J.B. Joo, J. Park, J. Yi, Preparation of polyelectrolyte-functionalized mesoporous silicas for the selective adsorption of anionic dye in an aqueous solution, J. Hazard. Mater. 168 (2009) 102–107.

[16] D.D. Asouhidou, K.S. Triantafyllidis, N.K. Lazaridis, K.A. Matis, Adsorption of Remazol Red 3BS from aqueous solutions using APTES- and cyclodextrin-modified HMS-type mesoporous silicas, Colloids Surf., A: Physicochem. Eng. Aspects 346 (2009) 83–90.

[17] A.R. Cestari, E.F.S. Vieira, G.S. Vieira, L.P. da Costa, A.M.G. Tavares, W. Loh, C. Airoldi, The removal of reactive dyes from aqueous solutions using chemically modified mesoporous silica in the presence of anionic surfactant—The temperature dependence and a thermodynamic multivariate analysis, J. Hazard. Mater. 161 (2009) 307–316.

[18] F.A. Pavan, S.L.P. Dias, E.C. Lima, E.V. Benvenutti, Removal of Congo red from aqueous solution by anilinepropylsilica xerogel, Dyes Pigm. 76 (2008) 64–69.

[19] A. Andrzejewska, A. Krysztafkiewicz, T. Jesionowski, Treatment of textile dye wastewater using modified silica, Dyes Pigm. 75 (2007) 116–124.

[20] B.K. Nandi, A. Goswami, M.K. Purkait, Adsorption characteristics of brilliant green dye on kaolin, J. Hazard. Mater. 161 (2009) 387–395.

[21] J.A.A. Sales, C. Airoldi, Epoxide silylant agent ethylenediamine reaction product anchored on silica gel-thermodynamics of cation-nitrogen interaction at solid/liquid interface, J. Non-Cryst. Solids 330 (2003) 142–149.

[22] J. Lin, J.A. Siddiqui, R.M. Ottenbrite, Surface modification of inorganic oxide particles with silane coupling agents and organic dyes, Polym. Adv. Technol. 12 (2001) 285–292.

[23] A. Ozcan, A.S. Ozcan, Adsorption of Acid Red 57 from aqueous solutions onto surfactant-modified sepiolite, J. Hazard. Mater. 125 (2005) 252–259.

[24] S. Senthilkumaar, P. Kalaamani, K. Porkodi, P.R. Varadarajan, C.V. Subburaam, Adsorption of dissolved reactive red dye from aqueous phase onto activated carbon prepared from agricultural waste, Bioresour. Technol. 97 (2006) 1618–1625.

[25] W.J. Weber, J.C. Morris, Kinetics of adsorption on carbon from solution, J. Sanitary Eng. Div. Am. Soc. Civ. Eng. 89 (1963) 31–60.

[26] S. Lagergren, Zur theorie der sogenannten adsorption geloster stoffe, K. Sven. Vetenskapsakad. Handl. 24 (1898) 1–39.

[27] Y.S. Ho, Adsorption of heavy metals from waste streams by peat, PhD thesis, The University of Birmingham, Birmingham, UK, 1995.

[28] I. Langmuir, The constitution and fundamental properties of solids and liquids. I. Solids, J. Am. Chem. Soc. 38 (1916) 2221–2295.

[29] I. Langmuir, The constitution and fundamental properties of solids and liquids. II. Liquids, J. Am. Chem. Soc. 39 (1917) 1848–1906.

[30] I. Langmuir, The adsorption of gases on plane surfaces of glass, mica and platinum, J. Am. Chem. Soc. 40 (1918) 1361–1403.

[31] H.M.F. Freundlich, Uber die adsorption in lasugen, Z. Phys. Chem. (Leipzig) 57A (1906) 385–470.

[32] M.J. Tempkin, V. Pyzhev, Recent modification to Langmiur isotherms, Acta Physiochim. USSR. 12 (1940) 217–222.

[33] Y.C. Kim, I. Kim, S.C. Rengraj, J. Yi, Arsenic removal using mesoporous alumina prepared via a templating method, Environ. Sci. Technol. 38 (2004) 924–931.

[34] G. Crini, C. Robert, F. Gimbert, B. Martel, O. Adam, F. De Giorgi, The removal of basic blue 3 from aqueous solutions by chitosan-based adsorbent: Batch studies, J. Hazard. Mater. 153 (2008) 96–106.
[35] M.N.V.R. Kumar, A review of chitin and Chitosan applications, React. Funct. Polym. 46 (2000) 1–27.
[36] N.M. Mahmoodi, F. Najafi, A. Neshat, Poly (amidoamine-co-acrylic acid) copolymer as a polymeric adsorbent: Synthesis, characterization, and its dye removal ability, Ind. Crop. Prod. 42 (2013) 119–125.
[37] N.M. Mahmoodi, F. Najafi, Synthesis, amine functionaliztion and dye removal ability of titania/silica nano-hybrid, Micropor. Mesopor. Mater. 156 (2012) 153–160.
[38] G. Crini, P.M. Badot, Application of chitosan, a natural aminopolysaccharide, for dye removal from aqueous solution by adsorption processes using batch studies: a review of recent literature, Prog. Polym. Sci. 33 (2008) 399–447.
[39] P.K. Dutta, K.D. Bhavani, N. Sharma, Adsorption for dyehouse effluent by low cost adsorbent (chitosan), Asian Textile J. 10 (2001) 57–63.
[40] M.S. Chiou, H.Y. Li, Adsorption behavior of reactive dye in aqueous solution on chemical cross-linked chitosan beads, Chemosphere 50 (2003) 1095–1105.
[41] S. Chatterjee, S. Chatterjee, B.P. Chatterjee, A.R. Das, A.K. Guha, Adsorption of a model anionic dye, eosin Y, from aqueous solution by chitosan hydrobeads, J. Colloid Interf. Sci. 288 (2005) 30–35.